The impact of light intensity on metabolomic profile of *Arabidopsis thaliana* wild type and *reticulata* mutant by NMR spectroscopy.

Tahereh Jafari[a, *], Moona Rahikainen[b], Elina Puljula[a], Jari Sinkkonen[a], Saijaliisa Kangasjärvi[b]

[a] Instrument Centre, Department of Chemistry, University of Turku, FI-20014 Turku, Finland

[b] Molecular Plant Biology, Department of Biochemistry, University of Turku, FI-20014 Turku, Finland

* Corresponding author: Tel: +358 29 450 3177. Fax: +358 29 450 5040. E-mail address: tahereh.jafari@utu.fi

Abstract

Light acclimation involves biochemical, metabolic and developmental adjustments that allow plants to cope with a vast range of growth environments. *Arabidopsis thaliana* mutants with photoperiod-dependent defects in leaf development and metabolism have been instrumental in deciphering the interlinked regulatory networks in plants. The *reticulata* (*re*) mutant displays dark green veins and pale green mesophyll tissues when grown under long day conditions. RE is a chloroplast envelope membrane protein of unknown function and is required for accurate primary metabolism and leaf development under long photoperiod, while its functional significance under short photoperiods has remained poorly understood. In the present study we assessed whether RE impacts primary metabolism or leaf development when *Arabidopsis* plants acclimate to different light intensities under short photoperiod. We show that growth under short day conditions annuls the metabolic and developmental defects of *re* mutants, suggesting that RE does not significantly modulate leaf development or primary metabolism under short photoperiod. Based on proton nuclear magnetic resonance spectroscopy (^{1}H NMR) and statistical analysis, however, the metabolite profiles of differentially light-acclimated short-day-grown plants differ with respect to sugars (glucose, fructose and sucrose), TCA cycle intermediates (fumaric, malic, citric and succinic acids) and fatty acids, which become more abundant under high light. Moreover, in contrast to isoleucine, leucine, valine, threonine, serine, tyrosine and phenylalanine, which show increased abundance in high-light-acclimated plants, the contents of alanine, glutamine, glutamic acid and aspartic acid are higher when plants grow under normal growth light. These findings indicate that NMR can detect high-light-induced metabolic adjustments that arise upon plant acclimation to light stress.

Key words *Arabidopsis thaliana, reticulata,* high light, ROS, ^{1}H NMR metabolites

1. Introduction

Plants respond to prevailing light conditions by eliciting metabolic and developmental adjustments that allow completion of their life cycle under a vast range of growth environments. Light is a key determinant of leaf development and optimizes the formation of photosynthetically active tissues, where the light-driven redox reactions occurring in chloroplasts convert solar energy into chemical form. Besides yielding photosynthetic end products, chloroplasts contribute to the biosynthesis of fatty acids, amino acids, vitamins, hormones and specialized secondary metabolites, which not only provide building blocks for the developing tissues, but also defend the plant against environmental stress agents. Imbalances in the light-driven redox chemistry, on the other hand, promote transient generation of reactive oxygen species (ROS), which serve important signaling functions under environmental challenges.

Appropriate development of leaf anatomy is critical for photosynthetic light harvesting, gas exchange and metabolic activities (González-Bayón et al., 2006; Pérez-Pérez et al., 2013) and leaf vasculature, especially the bundle sheath cells with specified metabolic properties, appear to mediate key functions in the underlying regulatory processes (Mullineaux et al., 2006; Yu et al., 2007; Cheng et al., 2006; Fryer et al., 2003; Kangajärvi et al., 2009). In *Arabidopsis* leaves, vascular tissues, especially the photosynthetic bundle sheath cells, display unique characteristics of ROS metabolism and accumulate hydrogen peroxide (H_2O_2) to elicit acclimation processes in high-light-illuminated leaves (Fryer et al., 2003).

In addition, metabolic reprogramming is a key element that allows plants to cope with light stress. Studies on *Arabidopsis* have illustrated high-light-induced alterations in carbon metabolism, presumably caused by altered photosynthetic activity and the associated activation of protective mechanisms (Jänkänpää et al., 2012; Wulff-Zottele et al., 2010).

Arabidopsis mutants have also been instrumental in revealing metabolic and regulatory cross-talk in plants. The *reticulata* (*re*) mutant, also identified as *lower cell density1* (*lcd1*; Barth and Conklin, 2003) and *radical-induced cell death2* (*rcd2*; Overmyer et al., 2008), shows accumulation of H_2O_2 in leaf veins and displays a reticulate phenotype with pale green mesophyll tissues when grown under long day conditions (González-Bayón et al., 2006; Li et al., 1995; Mollá-Morales et al., 2011). The *re* mutants display fewer mesophyll cells and smaller plastid size in the interveinal leaf regions as compared to wild type plants (Lundquist et al., 2014). The allelic *lcd1-1* mutant was identified in a screen for ozone (O_3) sensitivity, which was accompanied by bleaching of chlorophyll and accumulation of H_2O_2 along the vasculature (Barth and Conklin, 2003).

RE belongs to a family of six chloroplast envelope membrane proteins of unknown function and localizes primarily to bundle sheath cell chloroplasts along the vasculature (Pérez-Pérez et al., 2013). Extensive genetic and phenotypic analysis, together with transcriptomic and metabolomic profiling, revealed that RE family members are required to maintain amino acid homeostasis and accurate leaf development through partially over-lapping functions when plants grow under long day conditions (Pérez-Pérez et al., 2013). Extensive genetic and phenotypic analysis, together with transcriptomic and metabolomic profiling, revealed that RE family members are required to maintain amino acid homeostasis and accurate leaf development through partially over-lapping functions. Comparison of *Arabidopsis re* and *reticulata-related* (*rer*) mutants demonstrated that leaf reticulation associated with changes in ROS homeostasis and amino acid metabolism when plants grew under long day conditions (Pérez-Pérez et al., 2013). The nature of these molecular mechanisms, however, still remains unresolved.

While the importance of *re* on metabolic and regulatory interactions in long day conditions is relatively well established, its physiological significance under short day conditions in different light intensities has remained poorly understood.

The chemical composition and metabolites were measured by nuclear magnetic resonance spectroscopy (NMR). NMR is a technique based on exciting certain nuclei in a given sample with radio frequency pulse and measuring those frequency signals which have been emitted by the nuclei (Günther 2013). Proton nuclear magnetic resonance spectroscopy (^{1}H NMR) and statistical analysis can be used for exploring a large number of metabolites in the targeted object (Sekiyama et al., 2011).

Here we assessed how short day and growth light intensity impact morphological and metabolomic characteristics of *Arabidopsis* wild type and *re* mutant plants and analyzed their chemical composition and metabolites by nuclear magnetic resonance spectroscopy (NMR). We show that growth in short day conditions alleviates the phenotypical characteristics of *re* mutants, irrespective of the growth light intensity, and also the metabolite profiles of wild type and *re* mutants are alike. The metabolite profiles of differentially light-acclimated plants, however, display distinct differences, as evidenced by a number of primary metabolites and fatty acids that became more abundant in high-light-grown wild type and *re* plants as compared to plants grown under normal growth light. We conclude that exposure of plants to high light intensities triggers metabolic adjustments, presumably to enhance plant stress tolerance under challenging environmental cues. Under long photoperiods, RE is an essential component determining primary metabolism and leaf development.

Under short photoperiod, however, the functionality of RE is not critical in metabolic and developmental regulation in *Arabidopsis*.

2. Results and discussion

2.1. Phenotypes of wild type and reticulata plants under short day conditions

Phenotypic comparison of wild type and *re6* distinguished no reticulation in the rosette leaves of *re6* under short day and high light conditions (Fig. 1) and similar observations were made for the allelic *re4* and *re8* mutants (Fig. S1, Supplementary data). In line with the visual phenotypes, quantification of chlorophyll revealed no major differences between wild type and *re* when grown under growth light and high light (Table. S1). Hence, growth under short photoperiod annuls the developmental defect of *re* mutants regardless of the growth light intensity.

Next we explored the pattern of ROS accumulation in wild type and *re* mutant leaves with diaminobenzidine (DAB), which reacts with H_2O_2 causing appearance of a brown colored precipitation (Vanacker et al., 2000). DAB-staining of wild type and *re8* under short day and growth light revealed no detectable H_2O_2 accumulation in either of the genotypes (Fig. 1). Also under short day and high light, similar DAB-staining activity was observed between *re* and wild type (Fig. 1). For comparison, DAB-staining of wild type Col, *re4* and *re6* under long day and short day growth light and high light is presented in supplementary information (Fig. S2).

2.2. Metabolomic analysis of wild type and reticulata mutant under two different light intensities

The ^{1}H NMR signals from samples of 4 weeks old *Arabidopsis* wild type and *re* mutant grown under 130 µmol photons $m^{-2}s^{-1}$ (growth light) and 500 µmol photons $m^{-2}s^{-1}$ (high light) respectively, are shown in (Fig. 2). 25 metabolites were identified (Table 1) by comparing the chemical shifts and coupling constants of *Arabidopsis* proton spectra and reference compounds spectra, 1D-Tocsy (precisely for identification of sugars), 2D spectra (DQF-COSY, CH_2-edited HSQC and HMBC) and literature. No significant differences were observed between the metabolites of *Arabidopsis* wild type and *re* mutant at the same light intensities (Figs. 5A and 5B).

The signals in (0.85-0.92) ppm, (1.25-1.38) ppm, (1.53-1.64) ppm and (5.32- 5.39) ppm regions belonged to the fatty acids. The corresponding signals were more abundant in wild type and *re* mutant plants that were grown under 500 µmol photons $m^{-2}s^{-1}$ (high light). *Arabidopsis* fatty acids include

palmitic, linoleic, linolenic, hexadecatrienoic, oleic, hexadecenoic, stearic and hexadecadienoic acids (Yang and Ohlrogge, 2009). However, precise identification of the fatty acids was not possible based on the NMR data.

Table 1. Identified metabolites and ^{1}H NMR data of *Arabidopsis* wild type and *re* mutant under two different light intensities, 130 µmol photons $m^{-2}s^{-1}$ (growth light) and 500 µmol photons $m^{-2}s^{-1}$ (high light). Samples were measured in a mixture (1:1) of MeOD-d_4 and phosphate buffer (pH 6.2, D_2O, 25° C).

Metabolite	Position	δ_H (ppm)	Multiplicity	*J*(Hz)
Isoleucine	δ-CH_3	0.95	t	7.3
	γ'-CH_3	1.02	d	7.1
Leucine	δ-CH_3, δ'-CH_3	0.96-0.99	m	-
Valine	γ-CH_3	1.00	d	6.9
	γ'-CH_3	1.05	d	6.9
Threonine	γ-CH_3	1.33	d	6.5
Alanine	β-CH_3	1.48	d	7.2
Serine	CH	3.75-3.78	m	-
	CH_2	3.89-4.00	m	-
Succinic acid	H2, H2', H3, H3'	2.45	s	-
Glutamic acid	β-CH_2	2.02 - 2.17	m	-
	γ-CH_2	2.37-2.40	m	-
Glutamine	β-CH_2	2.08-2.18	m	-
	γ-CH_2	2.41-2.50	m	-
Malic acid	H3	2.42-2.46	m	-
	H3'	2.67-2.73	m	-
	H2	4.28	dd	3.5, 9.0
Citric acid	H3a, H3'a	2.53	d	15.9
	H3b, H3'b	2.70	d	15.9
Pyruvic acid	CH_3	2.34	s	-
Aspartic acid	β-CH	2.63	dd	9.2, 17.1
	β'-CH	2.81	dd	3.6,17.1
α -Glucose	H1	5.18	d	3.5
	H2	3.46	dd	3.7,9.7
	H3	3.69	t	9.2
	H4	3.36	t	9.37
	H6a	3.73	t	6.6
β - Glucose	H1	4.57	d	7.8
	H2	3.19	dd	1.4, 7.9
	H6a	3.87	dd	1.8,12.1
	H6b	3.70	dd	5.8, 12.1
Sucrose	H1	5.40	d	3.8
	H4	3.43	t	9.1
	H3'	4.17	d	8.6
	H4'	4.00-4.04	m	-
	H4,H3	4.06-4.08	m	-

β-D-Furoctofuranose	H1	3.55	d	12.4
	H6	4.02	dd	1.2,12.7
β-D-Fructopyranose	H5	3.93-3.95	m	-
	H4	3.85	dd	3.6,8.8
	H3	3.79	d	10.9
	H1	3.70	d	11.4
	H1’	3.51	d	11.4
Mannitol	H1	3.83	dd	2.4,11.6
	H2	3.63-3.67	m	-
	H3	3.78	d	7.8
Fumaric acid	H2, H3	6.53	s	-
Sinapoyl malate	CH-α	7.66	d	16.1
	CH-β	6.49	d	16.1
	H2,H6	7.00	s	-
	OCH_3-3/5	3.89	s	-
Tyrosine	δ-CH, δ’-CH	6.85	d	8.5
	ε-CH, ε’-CH	7.18	d	8.5
Phenylalanine	δ-CH, δ’-CH, ε-CH, ε’-CH, ζ-CH	7.32 - 7.43	m	-
Choline	N-$(CH_3)_3$	3.20	s	-
γ-aminobutyric acid	H4	3.00	t	7.2
	H3	1.86-1.95	m	-
	H2	2.30	t	7.2

[a] Multiplicity of the proton signals: s, singlet; d, doublet; dd, doublet of doublet; t, triplet; m, multiplet.

2.3. Comparison of wild type and reticulata at two different light conditions

Comparison between *Arabidopsis* wild type and *re* mutant grown under 130 µmol photons $m^{-2}s^{-1}$ (growth light) and 500 µmol photons $m^{-2}s^{-1}$ (high light) was performed by applying principal component analysis (PCA) model. The PCA scores plot (t[2] vs. t[1]) of the Pareto-scaled dataset (Fig. 3A) showed great goodness of fit ($R^2X_{(cum)} = 0.89$) and predictive ability $Q^2_{(cum)} = 0.84$, the first two principal components explained 77.30 % of the total variance. The model revealed a clear trend of discrimination between the first and the second component. In addition, the loadings line plot (Fig. 3B) of the corresponding PCA model indicated that the important variables that caused separation were alanine, glutamine, glutamic and aspartic acids on the negative side of the first principal component p[1] in *Arabidopsis* wild type and *re*, were grown

under 130 µmol photons $m^{-2}s^{-1}$ (growth light). In contrast, isoleucine, leucine, valine, threonine, serine, tyrosine, phenylalanine, choline, malic, fumaric, citric, γ-aminobutyric (GABA) and pyruvic acids, α-glucose, β-glucose, sucrose, β-D-furoctofuranose, β-D-fructopyranose, mannitol, sinapoyl malate and fatty acids were observed more concentrated on the positive side of the p[1] in wild type and *re* plants were grown under illumination at 500 µmol photons $m^{-2}s^{-1}$ (higher light intensity).

2.4. Comparison of wild type and reticulata mutant separately at two different light intensities

PCA model was accomplished (Fig. 4A) on *Arabidopsis* wild type samples that were grown under 130 µmol photons $m^{-2}s^{-1}$ (growth light) and 500 µmol photons $m^{-2}s^{-1}$ (high light). The model showed $R^2X_{(cum)} = 0.89$ and $Q^2_{(cum)} = 0.81$ respectively, the first two principal components explained 74.80 % of the total variation. A clear distinction was observed between the first and the second component. Wild type plants grown under 130 µmol photons $m^{-2}s^{-1}$ were observed on the positive side of the first component t[1] and wild type grown under 500 µmol photons $m^{-2}s^{-1}$ were placed at opposite side in the model. In addition, PCA analysis of *re* plants (Fig. 4B) grown under growth light and high light demonstrated $R^2X_{(cum)} = 0.92$, $Q^2_{(cum)} = 0.86$, the first two principal components explaining 81.75 % of the total variance. The model displayed separation between the groups. The *re* mutant grown under growth light were observed on the negative side of the second component and *re* samples that received high light on the positive side of the first component.

2.5. Comparison of wild type and reticulata mutant at the same light intensities

Comparison of wild type and *re* that were grown under 130 µmol photons $m^{-2}s^{-1}$ (growth light) was performed by PCA model (Fig. 5A). The first two principal components of the model ($R^2X_{(cum)} = 0.90$ and $Q^2_{(cum)} = 0.78$) explained 76.17% of the total variance. No statistical difference, was observed between wild type and *re* plant under growth light. Moreover, PCA model of *Arabidopsis*, wild type and *re* mutant (Fig. 5B) that received illumination at 500 µmol photons $m^{-2}s^{-1}$ (high light) showed $R^2X_{(cum)} = 0.84$ and $Q^2_{(cum)} = 0.74$, the first two principal components, covered 69.39% of the total variation. In addition, the model revealed no significant separation between wild type and *re* that were grown under high light.

2.6. Analysis of RE-promoter activity

In a previous study, Pérez-Pérez et al. (2013) showed that under long photoperiods leaf reticulation appeared in the *re* mutants. In our study, the absence of distinct differences between the metabolite profiles of wild type and *re* prompted us to assess the histological pattern of *RE* promoter activity in differentially light-acclimated plants under short days. Comparison of GUS-staining activities in the transgenic *RE$_{pro}$:GUS* reporter line under growth light (130 µmol photons $m^{-2}s^{-1}$) and high light (500 µmol photons $m^{-2}s^{-1}$) revealed no GUS activity in the bundle sheath cells under high light stress (Fig. 6B), while slight GUS staining was observed in plants that received normal growth light (Fig. 6A).

2.7. RE is not a key determinant of high light acclimation in Arabidopsis

Light acclimation involves a tightly interlinked regulatory network where biochemical, metabolic and developmental adjustments optimize plant physiology according to the prevailing light environment. Photoperiod and light intensity represent key parameters that modulate such regulatory programs in plants. Under long photoperiods, RE, a chloroplast envelope membrane protein of unknown function, is an essential molecular component required for accurate primary metabolism and leaf development in *Arabidopsis* (Pérez-Pérez et al., 2013). In this paper, we show that growth under short day conditions annuls the well-documented metabolic and developmental defects of *re* mutants (Pérez-Pérez et al., 2013), suggesting that RE does not significantly modulate leaf development or primary metabolism under short photoperiod (Figs 1 and 3; Table 1). These phenotypic properties of *re* mutants are in contrast with those observed in *ntrc*, which is deficient in a chloroplast NADPH-dependent thioredoxin reductase and shows reduced growth, altered amino acid profiles and a reticulate pattern of greening under short day conditions. Yet another example, *chlorophyll a/b binding protein underexpressed 1* (*cue1*) is deficient in a bundle-sheath-specific chloroplast phosphoenolpyruvate/phosphate (PEP) translocator, and exhibits drastic developmental disturbances in the mesophyll cells (Knappe et al. 2003). Even though the metabolic processes of chloroplasts appear to be tightly intertwined with the photoperiodic regulation of leaf development, the molecular mechanisms and regulatory interactions still remain poorly understood.

Day length has also been shown to condition stress-related ROS-dependent phenotypes. A well-known example is the *Arabidopsis cat2* mutant, which lacks CATALASE2 (CAT2) and hence accumulates photorespiratory H_2O_2 in leaf peroxisomes (Queval et al., 2007). Knock-out *cat2* plants show constitutive defense responses and cell death in long-day but not in short-day photoperiods (Queval et al., 2007, Chaouch et al., 2010). Notably, this response is genetically controlled via regulatory actions by protein phosphatase 2A regulatory subunit PP2A-B'γ (Chaouch et al., 2010; Li

et al., 2014). Similarly, *re* mutants show accumulation of ROS under long day conditions, while under short photoperiod this defect is not evident even under elevated light intensity (Fig. 1). Pérez-Pérez et al. (2013) indicated that *RE* is expressed in bundle sheath cells along leaf veins when the plants are grown under long day conditions. We found that *RE* promoter is not very active in short day conditions and barely detectable in plants grown under high light (Fig.6). Hence, it can therefore be assumed that the RE is not a key determinant of ROS signaling and acclimation in short-day photoperiods.

2.8. Growth under high light triggers metabolic adjustments in plants

Metabolic analysis has provided snapshots reflecting the concentrations and structures of metabolites in differentially stress-exposed plants, thereby shedding light on the complex metabolic interactions underlying stress resistance in plants (Chaouch et al., 2010; Li et al., 2014; Jänkänpää et al., 2012; Wulff-Zottele et al., 2010; Martins et al., 2014). Mass spectrometry based analysis of metabolic shifting in *Arabidopsis* upon acclimation to different light regimes showed that intermediates associated with tricarboxylic acid (TCA) cycle and sugar metabolism increased in abundance upon growth under high light, presumably to cope with elevated photosynthetic activity and the associated need to avoid oxidative stress (Jänkänpää et al., 2012; Wulff-Zottele et al., 2010). By a different technical approach using NMR analysis, we also detected accumulation of sugars (glucose, fructose derivatives and sucrose) and organic acids involved in the TCA cycle (fumaric, malic, citric and succinic acids) in high-light-grown plants (Fig. 3B). Notably, statistical analysis of the NMR spectra did not indicate any significant differences between wild type *Arabidopsis* and the *reticulata* mutants (Fig. 3). Moreover, in contrast to increased contents of isoleucine, leucine, valine, threonine, serine, tyrosine and phenylalanine, the NMR analysis displayed lower concentrations of alanine, glutamine, glutamic acid and aspartic acid in high-light-grown *Arabidopsis* wild type and *re* mutants as compared to plants grown under normal growth light (Fig. 3B).

Amino acids are central metabolic components that form points of cross-talk between primary and secondary metabolism. It is therefore conceivable that the contents of individual amino acids are prone for alterations upon environmental challenges, and that these fluctuations can be greatly affected by both up-stream and down-stream activities within the metabolic networks. Hence, the apparent differences between the existing reports on high-light-induced alterations in amino acid profiles likely arise from the usage of different plant species and different experimental setups (Fig 4, Jänkäpää et al., 2012, Martins et al., 2014). Even so, light plays an important role in the regulation

of nitrate assimilation and the down-stream pathways of amino acid metabolism. Muller et al. (2017) reported that nitrate levels in *Arabidopsis* decrease under high light, and that N-homeostasis is influenced by the pools of glutamine and glutamic acid. A decrease in nitrate concentration was also observed in lettuce leaves under high light and low nitrogen conditions by Fu et al. (2017), who found that the nitrate concentration peaked under a relatively low light intensity of 60 μmol photons $m^{-2}s^{-1}$. In their report, Fu et al. (2017) concluded that increased availability of photochemical energy accelerates assimilation of free nitrate into amino acids under high light. The impact of down-stream metabolic activities on metabolite contents was further illustrated by Woodrow et al. (2017), who found that exposure of wheat seedlings to a combination of high light and salinity stress resulted in a decline in glutamate concentration, presumably due to utilization of glutamate as a nitrogen donor for biosynthesis of other amino acids or in decarboxylation process to produce γ-aminobutyric acid (GABA). With respect to stress tolerance, Woodrow et al. (2017) revealed that fine-tuning of only a few specific primary metabolites, including GABA, amides, minor amino acids and hexoses was sufficient to remodel the metabolic and defensive processes, hence playing a key role in the responses to simultaneous high light and salinity stress. Evidently, high light illumination may promote the accumulation of metabolites that alleviate oxidative stress and enhance the photosynthetic production potential.

Martins et al. (2014) suggested that high-light-induced increases in metabolite contents may significantly impact plant protection: 1) Sugars, polyols and amino acids display protective effects against osmotic stress and may also hold ROS scavenging activities, 2) Serine, glutamine and glycine maintain photorespiratory metabolism that can quench excess excitation energy in chloroplasts, 3) Alanine associates with the biosynthesis of CoA and forms a main precursor in both primary and secondary metabolism, 4) Ascorbate is an essential antioxidant, 5) Shikimate pathway and accumulation of aromatic amino acids provide precursors for protective secondary metabolites, and 6) Polyamines protect plants through so far unknown mechanisms. The currently available data on plant metabolomics highlights the importance of light intensity on the regulation of metabolite contents in *Arabidopsis* leaves. Hence, plant exposure to high light intensities triggers metabolic adjustments that may essentially enhance plant resilience and optimize their productivity under challenging environmental cues.

3. Experimental

3.1. Plant material

Homozygote *reticulata* (*re4*, *re6* and *re8*) mutants and the transgenic *RE$_{pro}$:GUS* reporter line were described previously (Pérez-Pérez et al., 2013). For biochemical analysis, *Arabidopsis* wild type ecotype Columbia (Col), *re* mutants and *RE$_{pro}$:GUS* in wild type background were grown under 130 µmol photons $m^{-2}s^{-1}$ (growth light), at 22 ºC with 50% humidity at an 8-hour light period for two weeks. Subsequently, the seedlings were either kept under growth light or transferred to 500-600 µmol photons $m^{-2}s^{-1}$ (high light) for two weeks. Metabolite analysis of wild type and *re* grown under the two different light intensities were conducted after harvesting the four-week-old rosette leaves four hours into the light period. 21 biological replicates per line were collected for plants grown under growth light and 26 replicates were collected for high-light-grown plants. Each sample contained a pool of 3 individual freeze dried plants, in order to achieve 15 mg of dry powder of *Arabidopsis* required for NMR sample preparation. The plant material was immediately frozen in liquid nitrogen to prevent any biochemical alteration and stored at -80º C until dried using a freeze dryer.

3.2. Analysis of RE promoter activity

4 weeks old *RE$_{pro}$:GUS* plants (Pérez-Pérez et al., 2013), were grown under two different light intensities, 130 µmol photons $m^{-2}s^{-1}$ (growth light) and 500 µmol photons $m^{-2}s^{-1}$ (high light). After harvesting, the rosettes were placed on petri dishes and fixed in ice cold acetone and thereafter washed twice with sodium phosphate buffer (pH 7.2). The staining buffer (50 mM sodium phosphate buffer (pH 7.2), 1 mM X-Gluc) was added to the petri dishes and samples were incubated at 37 ºC overnight. Thereafter, the staining buffer was removed and the samples were washed with Milli-Q water. Finally, the rosettes were cleared by incubation in increasing concentrations of ethanol (30%, 50%, 70% and 100%) and photographed.

3.3. DAB-staining of H_2O_2

Foliar H_2O_2 was detected by using diaminobenzidine (DAB) (Sigma-Aldrich) as a substrate (Thordal-Christensen et al., 1997) with the modifications described by Kangasjärvi et al. (2008). Briefly, the rosettes were excised at the end of the light period, and incubated in 0.1 mg/ml solution of DAB (10 mM MES-KOH buffer, pH 5.6) overnight in darkness. At the onset of the light period, the dishes

were transferred to growth light for 2 h, and also the rosettes incubated under high light for 2 h. Thereafter the rosettes were incubated in 96% (v/v) ethanol until chlorophyll was bleached, and photographed.

3.4. Quantification of Chlorophyll

Foliar chlorophyll content was determined by punching two leaf discs, 25.13 mm^2 in diameter, into 1 mL of dimethylformamide. The leaf discs were incubated overnight at 4º C in darkness, and the chlorophyll content was measured spectrophotometrically according to Inskeep and Bloom (1985).

3.5. Preparation of NMR samples

Arabidopsis wild type and *re* mutant samples were freeze dried in a CHRiST CHRiST, BETA 1-8 LD_{plus} / BETA 2-8 LD_{plus} freeze dryer for 72 hours. Freeze dried samples were grinded to obtain fine powder and stored in – 18 ºC freezer before the extraction. 15 mg of dry powder was mixed with 0.8 ml solution (v/v 1/1) of MeOD-d_4 (deuterated methanol) and 0.1 M phosphate buffer in D_2O (pH 6.2, 3 mM TSP, 2 mM NaN_3). Sodium azide (NaN_3) was used to prevent bacterial growth in NMR samples. Samples were vortexed for 15 min and centrifuged (9000 rpm, 15 min, 22º C). 0.6 ml of the supernatant was pipetted in to the 5 mm NMR tubes (Bruker, Code-no. 5x103.5-S-0, 38) to be measured with NMR.

3.6. Chemicals

MeOD-d_4 (99.80 % D), D_2O (99.90 % D) and 3-(trimethylsilyl) propionic acid sodium salt (TSP) (98% D) were purchased from Euriso-top, K_2HPO_4, KH_2PO_4 and NaN_3 (99.5%) from Sigma Aldrich.

Sodium phosphate buffer Included (Na_2HPO_4 and NaH_2PO_4), Dimethylformamide (DMF), Acetone, X-Gluc (5-bromo-4-chloro-3-indolyl beta-D-glucuronide cyclohexamine salt) and ethanol.

3.7. NMR spectroscopy

The measurement of spectra was accomplished with Bruker Avance III 600 spectrometer (Bruker BioSpin AG, Fällanden, Switzerland) with a triple head Prodigy TCI 5 mm inverse nitrogen cooled cryprobe operating at 600.16 MHz for ^1H and at 150.92 MHz for ^{13}C and equipped with precooled SampleJet sample changer. Presaturation proton experiment (*zgpr* pulse programme) was utilized to suppress residual signal of H_2O at 4.81 ppm. Measurement was proceeding with 256 scans at 25º C, an acquisition time of 5.453 s, a relaxation delay of 5.0 s and a 90º pulse of 8 µs. Free induction decays (FIDs) consisted of 128 K data points and spectral width was 12,000 Hz. Additionally, a set of other NMR experiments, such as: DQFCOSY (*cosygpmfqf*), 1D-TOCSY(*selmlgp*), NOESY

(*noesygp*), CH_2-edited ^{1}H-^{13}C HSQC (*hsqcedetgpsisp2*) and ^{1}H-^{13}C HMBC (*hmbcgplpndqf*), were applied to the selected samples to aid the identification of compounds (Figs. S3 – S8, Supplementary data).

3.8. Data processing

The data was transferred to the TopSpin 3.2 software (Bruker BioSpin GmbH, Rheinstetten, Germany). The baselines and phases of the spectra were corrected automatically and calibrated to the TSP signal at 0.00 ppm. AMIX software (Bruker BioSpin GmbH) was used to bin the spectra from 10.0 to – 0.5 ppm into an equal width of 0.02 ppm per bin. Each bin represents a numeral integral value of a specific spectral area. As NMR is a quantitative method, the peak integral is proportional to the number of protons responsible for the signal, but also to the total concentration of the compound. Thus, the bins can be used to compare the relative concentrations of compounds.

The spectra were scaled into the reference region from – 0.12 to + 0.12. The bin of residual signals of water from 4.76 to 4. 87 ppm and methanol from 3.30 to 3.33 ppm were excluded. The integration mode was chosen as positive intensities. The binned spectra were exported into the Microsoft Excel 2013.

3.9. Data analysis

Multivariate data analysis was obtained by SIMCA-P+ 12.0.1 software (Umetrics AB, Umeå, Sweden) to interpret and evaluate datasets. Principal component analysis (PCA) was utilized as the multivariate method to view the most variation in the datasets without predefined grouping. PCA is an unsupervised technique to observe general conspectus (Rajalahti and Kvalheim, 2011). The datasets were Pareto-scaled. In addition, partial least squares discriminant analysis (PLS-DA) was tested to emphasize separation of the groups. PLS-DA is a supervised method to distinguish the difference between predefined groups (Chevallier et al., 2006). However, it didn't contribute further information and is not explained here in more detail.

3.10. Identification of the metabolites

The metabolites were identified with the aid of reference compounds (confirmation of identified metabolites was based on comparing proton spectra before and after adding the reference compound to certain samples), literature, set of two-dimensional experiments (with the specific samples) and

410 metabolite databases, such as Human Metabolome Database (HMDB; http://www.hmdb.ca/)
411 (Wishart et al., 2012).

412

Acknowledgments: Lassi Raivonen is acknowledged for excellent technical assistance. This work was financially supported by the Turku University Foundation, Alfred Kordelin foundation, the Academy of Finland (project numbers 307335 and 307719), the Department of Chemistry, University of Turku.

Figure Captions

Fig. 1. (Up) *Arabidopsis* wild type COL and *reticulata* (*re6*) mutant grown under short day, 130 µmol photons $m^{-2}s^{-1}$ (growth light) or 500 µmol photons $m^{-2}s^{-1}$ (high light). **(Below)** DAB-staining of H_2O_2 included *Arabidopsis* wild type (COL) and *reticulata* (*re6*) under short day and 130 µmol photons $m^{-2}s^{-1}$; Wild type (COL) and *re* under short day and 600 µmol photons $m^{-2}s^{-1}$.

Fig.2. ^{1}H NMR of *Arabidopsis* grown under 130 µmol photons $m^{-2}s^{-1}$ (growth light; wild type black and *reticulata* (*re6*) red) and 500 µmol photons $m^{-2}s^{-1}$ (high light; wild type blue and *reticulata* (*re6*) green).

Fig. 3. A PCA scores plot t[2] vs. t[1], observations colored according to, *Arabidopsis*, wild type and *reticulata* (*re6*) mutant that grown up under 130 µmol photons $m^{-2}s^{-1}$ (growth light) and wild type and *reticulata* (*re6*) plants that grown under 500 µmol photons $m^{-2}s^{-1}$ (high light), ($R^2X_{(cum)}$ = 0.89 and $Q^2_{(cum)}$ = 0.84); **B** The loadings line plot vs. primary variable ID.

Fig. 4. A PCA scores plot t[2] vs. t[1], observations colored due to, *Arabidopsis*, wild type that grown up under 130 µmol photons $m^{-2}s^{-1}$ (growth light) and wild type that grown under 500 µmol photons $m^{-2}s^{-1}$ (higher light), ($R^2X_{(cum)}$ = 0.89 and $Q^2_{(cum)}$ = 0.81); **B** PCA scores plot t[2] vs. t[1], observations colored according to, *Arabidopsis*, *reticulata* (*re6*) mutant that grown up under 130 µmol photons $m^{-2}s^{-1}$ (growth light) and *reticulata* (*re6*) plants that received higher light intensity (500 µmol photons $m^{-2}s^{-1}$) respectively, ($R^2X_{(cum)}$ = 0.92 and $Q^2_{(cum)}$ = 0.86).

Fig. 5. A PCA scores plot t[2] vs. t[1], observations colored in order to, *Arabidopsis*, wild type and *reticulata* (*re6*) mutant that grown up under 130 µmol photons $m^{-2}s^{-1}$ (growth light), ($R^2X_{(cum)}$ = 0.90 and $Q^2_{(cum)}$ = 0.78); **B** PCA scores plot t[2] vs. t[1], observations colored according to, *Arabidopsis*, wild type and *reticulata* (*re6*) mutant that grown under 500 µmol photons $m^{-2}s^{-1}$ (high light), ($R^2X_{(cum)}$ = 0.84 and $Q^2_{(cum)}$ = 0.74).

Fig. 6 GUS activity of 4 weeks old *Arabidopsis* (under short days), **A** RE_{pro}*:GUS* grown under 130 µmol photons $m^{-2}s^{-1}$; **B** RE_{pro}*:GUS* that received light intensity at 500 µmol photons $m^{-2}s^{-1}$ (high light) for two weeks.

Fig.1.

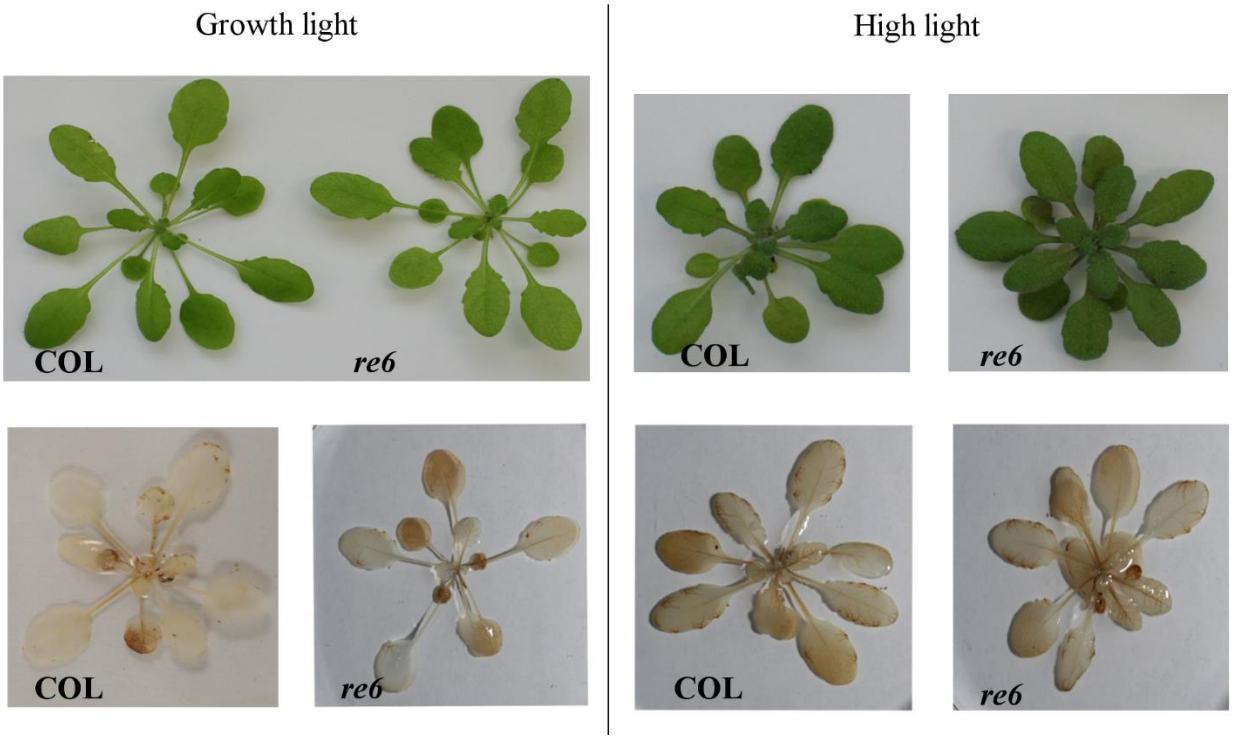

Fig.2.

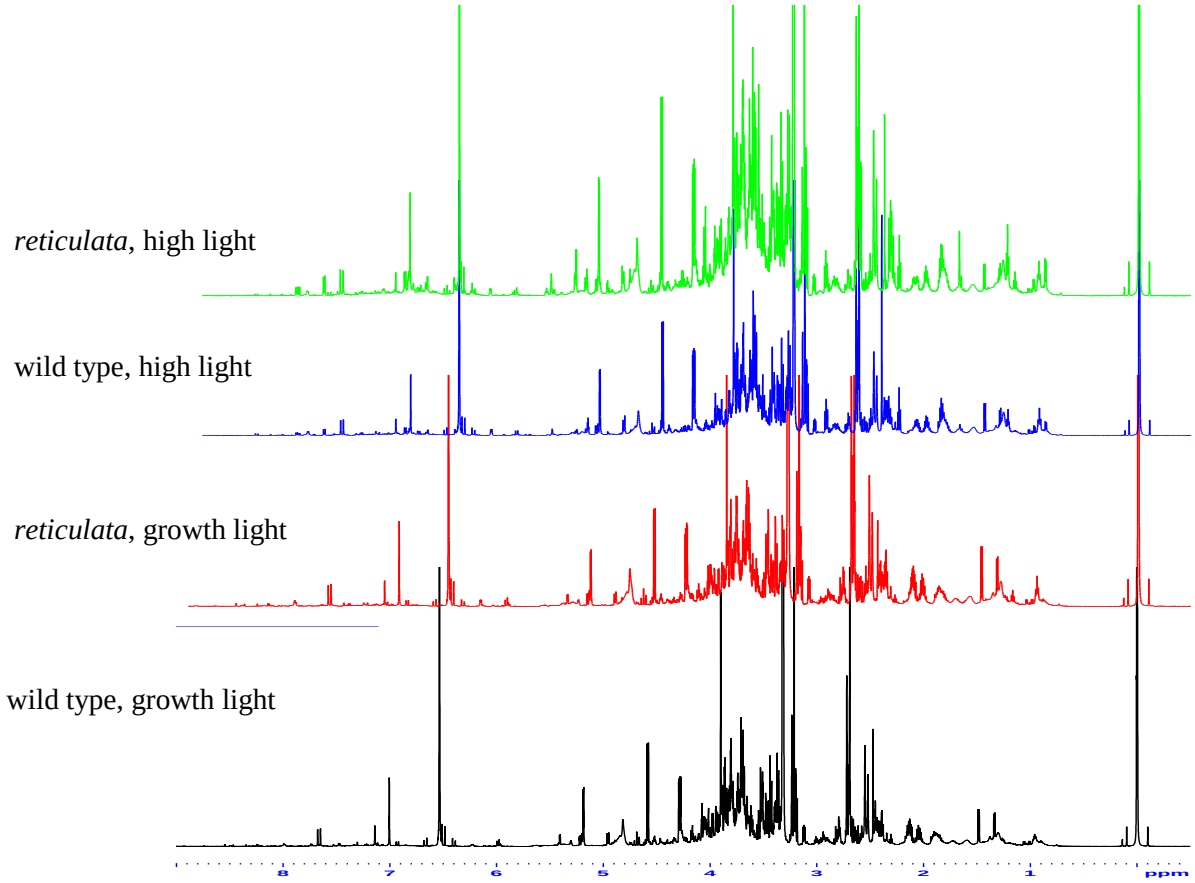
reticulata, high light
wild type, high light
reticulata, growth light
wild type, growth light
8
7
6
5
4
3
2
1
ppm

Fig.3.

A)

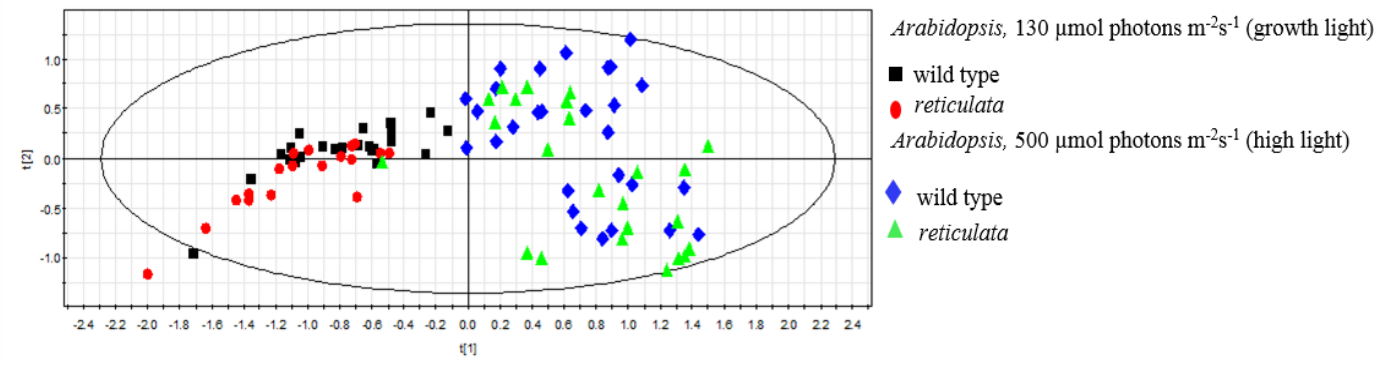
t[2]
t[1]
Arabidopsis, 130 µmol photons m-2s-1 (growth light)
wild type
reticulata
Arabidopsis, 500 µmol photons m-2s-1 (high light)
wild type
reticulata

B)

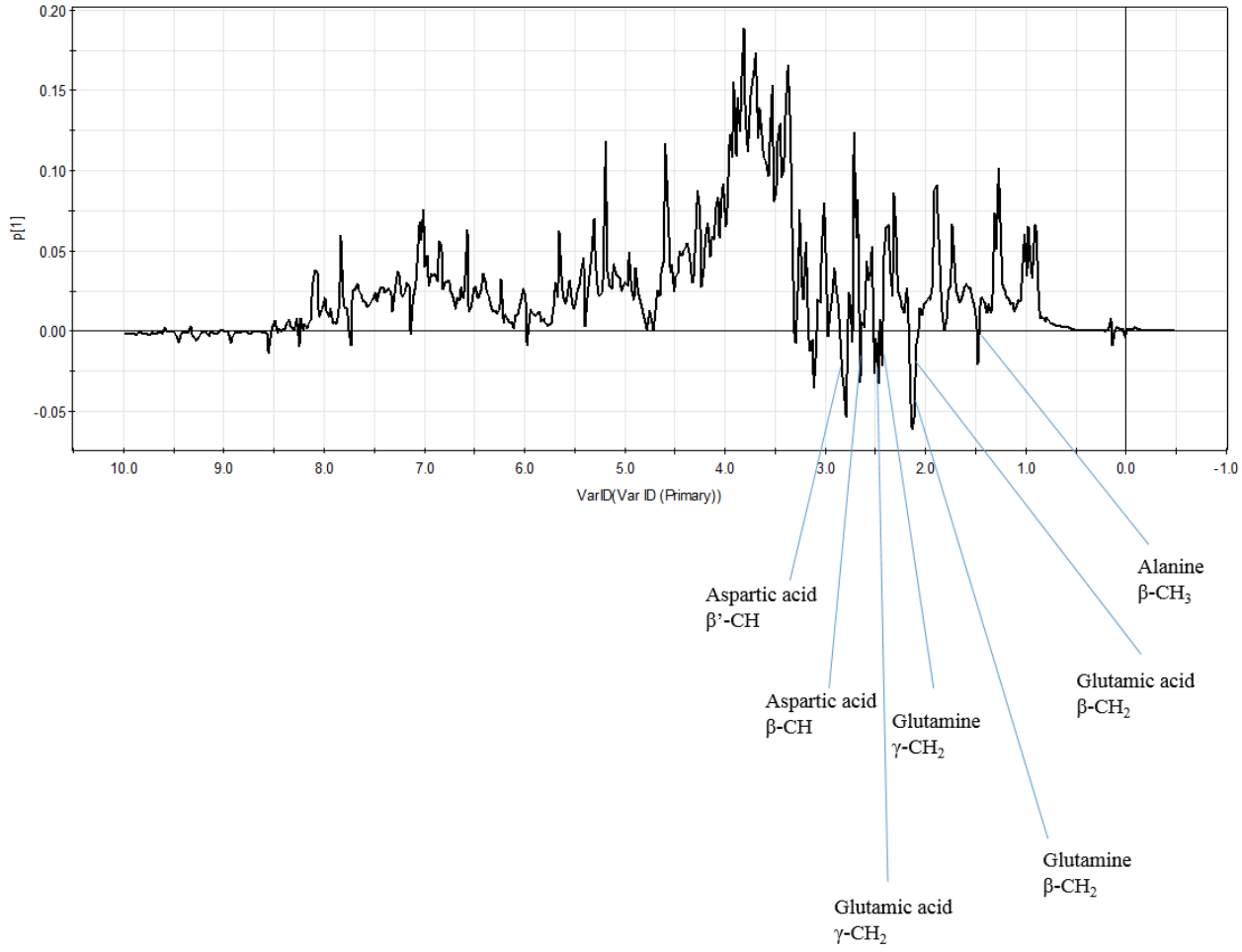
p[1]
VarID(Var ID (Primary))
Aspartic acid β'-CH
Aspartic acid β-CH
Glutamine γ-CH2
Glutamic acid γ-CH2
Glutamine β-CH2
Glutamic acid β-CH2
Alanine β-CH3

Fig. 4.

A)

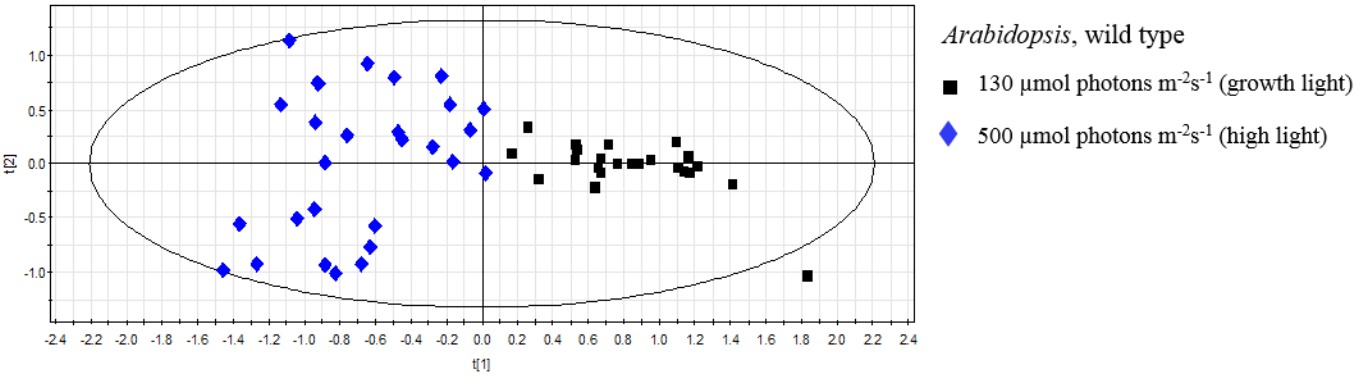
t[2]
t[1]
Arabidopsis, wild type
130 µmol photons m-2s-1 (growth light)
500 µmol photons m-2s-1 (high light)

B)

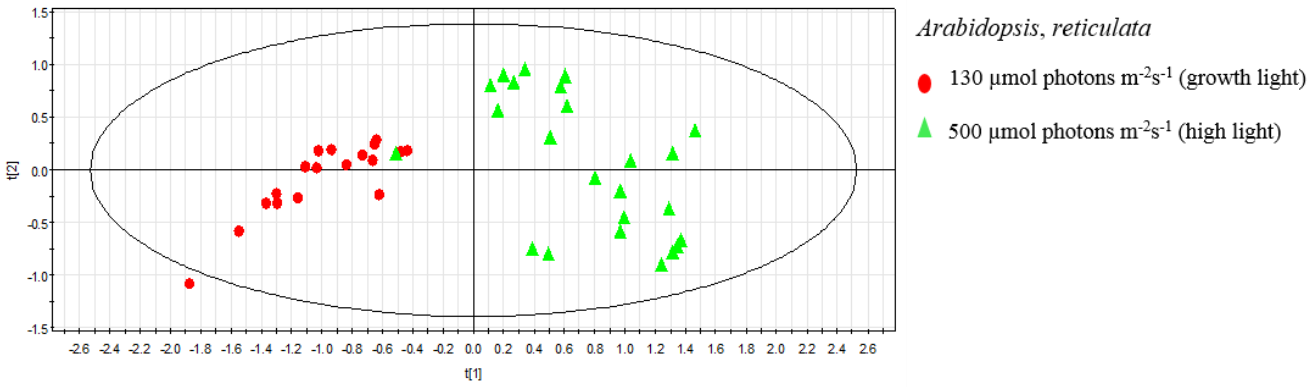
t[2]
t[1]
Arabidopsis, *reticulata*
130 µmol photons m-2s-1 (growth light)
500 µmol photons m-2s-1 (high light)

Fig.5.

A)

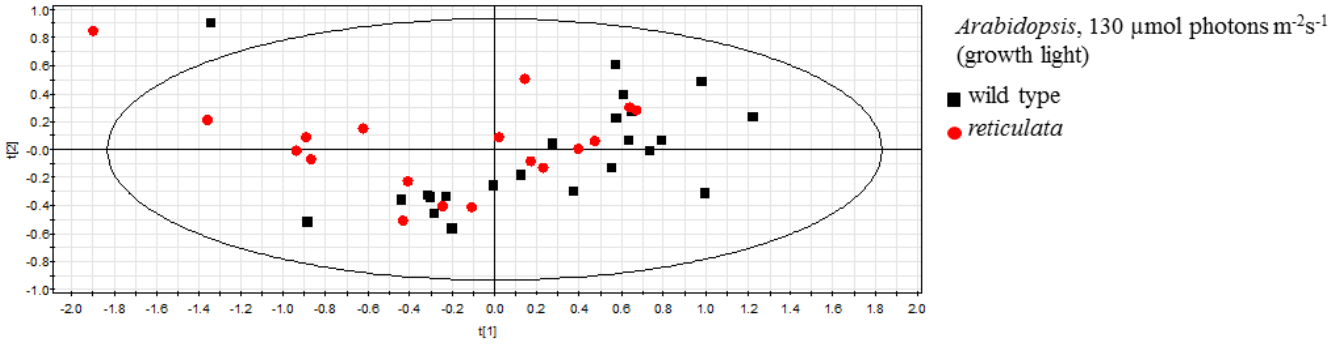
t[2]
t[1]
Arabidopsis, 130 µmol photons m-2s-1 (growth light)
wild type
reticulata

B)

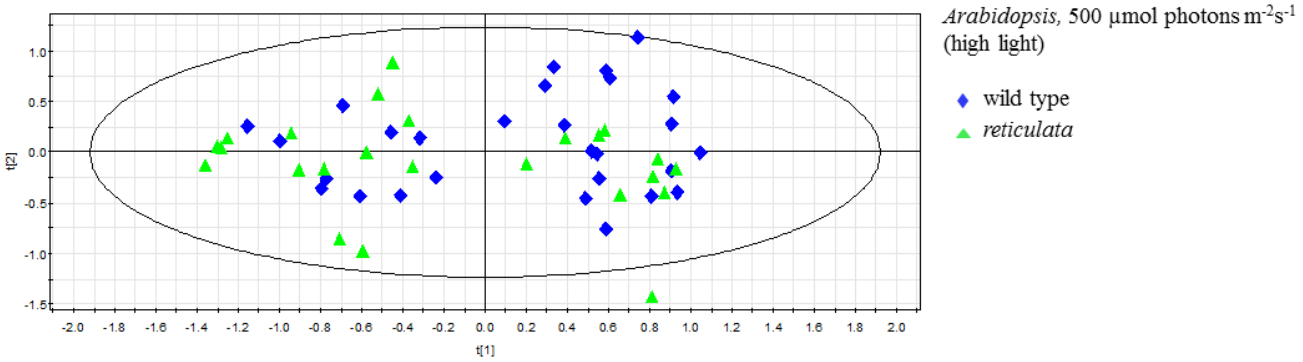
t[2]
t[1]
1.0
0.5
0.0
-0.5
-1.0
-1.5
-2.0 -1.8 -1.6 -1.4 -1.2 -1.0 -0.8 -0.6 -0.4 -0.2 0.0 0.2 0.4 0.6 0.8 1.0 1.2 1.4 1.6 1.8 2.0
Arabidopsis, 500 µmol photons $m^{-2}s^{-1}$ (high light)
wild type
reticulata

Fig.6.

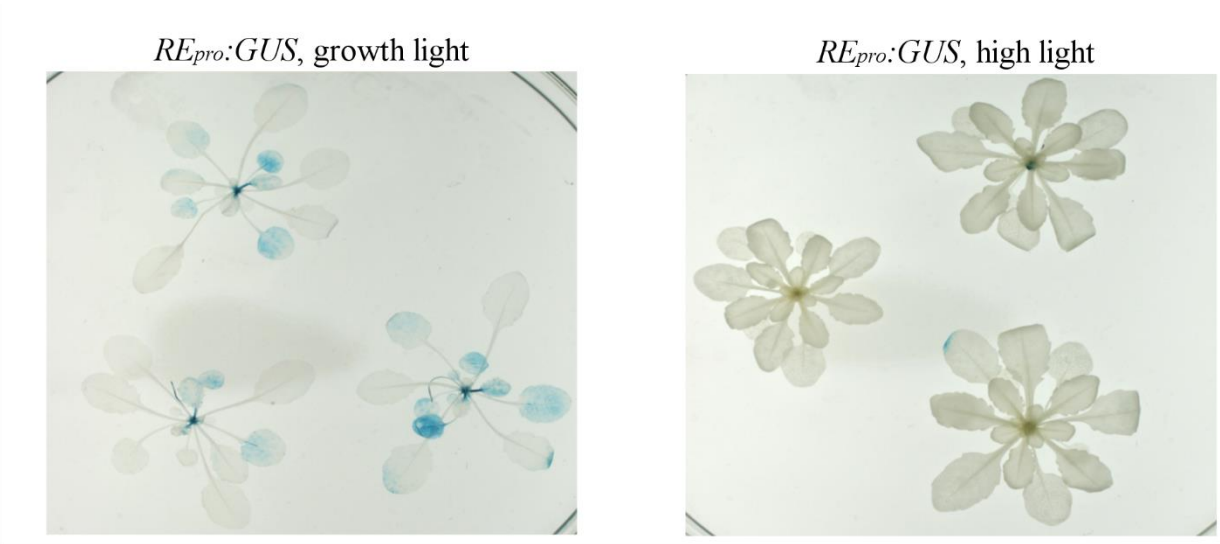
RE$_{pro}$*:GUS*, growth light
RE$_{pro}$*:GUS*, high light

References

Barth, C., Conklin, PL., 2003. The lower cell density of leaf parenchyma in the *Arabidopsis thaliana* mutant *lcd1-1* is associated with increased sensitivity to ozone and virulent *Pseudomonas syringae*. Plant J. 35, 206–218.

Chaouch, S., Queval, G., Vanderauwera, S., Mhamdi, A., Vandorpe, M., Langlois-Meurinne, M., Van Breusegem, F., Saindrenan, P., Noctor, G., 2010. Peroxisomal hydrogen peroxide is coupled to biotic defense responses by ISOCHORISMATE SYNTHASE1 in a day length-related manner. J Plant Physiol. 153, 1692–1705.

Cheng, N.H., Liu, J.Z., Brock, A., Nelson, R.S., Hirschi, K.D., 2006. AtGRXcp, an *Arabidopsis* chloroplastic glutaredoxin, is critical for protection against protein oxidative damage. J Biol Chem. 281, 26280–26288.

Chevallier, S., Bertrand, D., Kohler, A., Courcoux, P., 2006. Application of PLS-DA in multivariate image analysis. J Chemom. 20, 221–229.

Fryer, M.J., Ball, L., Oxborough, K., Karpinski, S., Mullineaux, P.M., Baker, N.R., 2003. Control of Ascorbate Peroxidase 2 expression by hydrogen peroxide and leaf water status during excess light stress reveals a functional organisation of *Arabidopsis* leaves. Plant J. 33, 691–705.

Fu, Y., Li, H.Y., Yu, J., Liu, H., Cao, Z.Y., Manukovsky, N.S., Liu, H., 2017. Interaction effects of light intensity and nitrogen concentration on growth, photosynthetic characteristics and quality of lettuce (*Lactuca sativa L. Var. youmaicai*). Sci Hortic. 214, 51–57.

González-Bayón, R., Kinsman, E.A., Quesada, V., Vera, A., Robles, P., Ponce, M.R., Pyke, K.A., Micol, J.L., 2006. Mutations in the RETICULATA gene dramatically alter internal architecture but have little effect on overall organ shape in *Arabidopsis* leaves. J Exp Bot. 57, 3019–3031.

Günther, H., 2013. NMR spectroscopy: basic principles, concepts and applications in chemistry. John Wiley & Sons.

Inskeep, W. P., Bloom, P. R., 1985. Extinction coefficients of chlorophyll a and b in N, N-dimethylformamide and 80% acetone. J Plant physiol. *77*, 483–485.

Jänkänpää, H.J., Mishra, Y., Schröder, W.P., Jansson, S., 2012. Metabolic profiling reveals metabolic shifts in *Arabidopsis* plants grown under different light conditions. J Plant Cell Environ. 35, 1824–1836.

Kangasjärvi, S., Lepistö, A., Hännikäinen, K., Piippo, M., Luomala, E.M., Aro, E.M., Rintamäki, E., 2008. Diverse roles for chloroplast stromal and thylakoid-bound ascorbate peroxidases in plant stress responses. Biochem J. 412, 275–285.

Kangasjärvi, S., Nurmi, M., Tikkanen, M., ARO, E., 2009. Cell-specific mechanisms and systemic signalling as emerging themes in light acclimation of C3 plants. J Plant Cell Environ.32, 1230–1240.

Knappe, S., Lottgert, T., Schneider, A., Voll, L., Flugge, U.I., Fischer, K., 2003. Characterization of two functional *phosphoenolpyruvate/phosphate translocator* (*PPT*) genes in *Arabidopsis* – *AtPPT1* may be involved in the provision of signals for correct mesophyll development. Plant J. 36, 411–420.

595 Li, H., Culligan, K., Dixon, R.A., Chory, J., 1995. CUE1: a mesophyll cell-specific positive regulator of light-
596 controlled gene expression in *Arabidopsis*. Plant Cell. 7, 1599–1610.
597
598 Li, S., Mhamdi, A., Trotta, A., Kangasjärvi, S., Noctor, G., 2014. The regulatory subunit B′ γ of protein
599 phosphatase 2A acts downstream of oxidative stress in the control of salicylic acid responses by peroxisomal
600 H_2O_2. New Phytol. 202, 145–160.
601
602 Lundquist, P.K., Rosar, C., Bräutigam, A., Weber, A.P., 2014. Plastid signals and the bundle sheath: mesophyll
603 development in reticulate mutants. Mol Plant. 7, 14–29.
604
605 Martins, S.C., Araújo, W.L., Tohge, T., Fernie, A.R., DaMatta, F.M., 2014. In high-light-acclimated coffee
606 plants the metabolic machinery is adjusted to avoid oxidative stress rather than to benefit from extra light
607 enhancement in photosynthetic yield. PloS one. 9, e94862.
608
609 Mullineaux, P.M., Karpinski, S., Baker, N.R., 2006. Spatial dependence for hydrogen peroxide-directed
610 signaling in light-stressed plants. Plant Physiol. 141, 346–350.
611
612 Müller, S.M., Wang, S., Telman, W., Liebthal, M., Schnitzer, H., Viehhauser, A., Sticht, C., Delatorre, C.,
613 Wirtz, M., Hell, R., 2017. The redox-sensitive module of cyclophilin 20-3, 2-cysteine peroxiredoxin and
614 cysteine synthase integrates sulfur metabolism and oxylipin signaling in the high light acclimation response.
615 Plant J. 91, 995–1014.
616
617 Mollá-Morales, A., Sarmiento-Mañús, R., Robles, P., Quesada, V., Pérez-Pérez, J.M., González-Bayón, R.,
618 Hannah, M.A., Willmitzer, L., Ponce, M.R., Micol, J.L., 2011. Analysis of *ven3* and *ven6* reticulate mutants
619 reveals the importance of arginine biosynthesis in *Arabidopsis* leaf development. Plant J. 65, 335–345.
620
621 Overmyer, K., Kollist, H., Tuominen, H., Betz, C., Langebartels, C., Wingsl, G., Kangasjärvi, S., Brader, G.,
622 Mullineaux, P., Kangasjärvi, J., 2008. Complex phenotypic profiles leading to ozone sensitivity in *Arabidopsis*
623 *thaliana* mutants. Plant Cell Environ. 31, 1237–1249.
624
625 Pérez-Pérez, J. M., Esteve-Bruna, D., González-Bayón, R., Kangasjärvi, S., Caldana, C., Hannah, M. A.,
626 Willmitzer, L., Ponce, M .R., Micol, J.L., 2013. Functional redundancy and divergence within the *Arabidopsis*
627 RETICULATA-RELATED gene family. Plant Physiol.162, 589–603.

628 Queval, G., Issakidis-Bourguet, E., Hoeberichts, F.A., Vandorpe, M., Gakiere, B., Vanacker, H., Miginiac-
629 Maslow, M., Van Breusegem ,F., Noctor, G., 2007. Conditional oxidative stress responses in the *Arabidopsis*
630 photorespiratory mutant *cat2* demonstrate that redox state is a key modulator of daylength-dependent gene
631 expression, and define photoperiod as a crucial factor in the regulation of H_2O_2-induced cell death. Plant J.
632 52,640–657.

633 Rajalahti, T., Kvalheim, O.M., 2011. Multivariate data analysis in pharmaceutics: a tutorial review. Int J
634 Pharmaceutics. 417, 280–290.
635
636 Sekiyama, Y., Chikayama, E., Kikuchi, J., 2011. Evaluation of a semipolar solvent system as a step toward
637 heteronuclear multidimensional NMR-based metabolomics for 13C-labeled bacteria, plants, and animals. Anal
638 Chem. 83, 719–726.
639

Thordal-Christensen, H., Zhang, Z., Wei, Y., Collinge, D.B., 1997. Subcellular localization of H_2O_2 in plants. H_2O_2 accumulation in papillae and hypersensitive response during the barley—powdery mildew interaction. Plant J. 11, 1187–1194.

Vanacker, H., Carver, T.L., Foyer, C.H., 2000. Early H_2O_2 accumulation in mesophyll cells leads to induction of glutathione during the hyper-sensitive response in the barley-powdery mildew interaction. Plant Physiol . 123, 1289–1300.

Wishart, D.S., Jewison, T., Guo, A.C., Wilson, M., Knox, C., Liu, Y., Djoumbou, Y., Mandal, R., Aziat, F., Dong, E., 2012. HMDB 3.0—the human metabolome database in 2013. Nucleic acids research, gks1065.

Woodrow, P., Ciarmiello, L.F., Annunziata, M.G., Pacifico, S., Iannuzzi, F., Mirto, A., D'Amelia, L., Dell'Aversana, E., Piccolella, S., Fuggi, A., 2017. Durum wheat seedling responses to simultaneous high light and salinity involve a fine reconfiguration of amino acids and carbohydrate metabolism. Physiol Plant. 159, 290–312.

Wulff-Zottele, C., Gatzke, N., Kopka, J., Orellana, A., Hoefgen, R., Fisahn, J., Hesse, H., 2010. Photosynthesis and metabolism interact during acclimation of *Arabidopsis thaliana* to high irradiance and sulphur depletion. Plant Cell Environ. 33, 1974–1988.

Yang, Z., Ohlrogge, J.B., 2009. Turnover of fatty acids during natural senescence of *Arabidopsis*, *Brachypodium*, and switchgrass and in *Arabidopsis* β-oxidation mutants. Plant Physiol. 150, 1981–1989.

Yu, F., Fu, A., Aluru, M., Park, S., Xu, Y., Liu, H., Liu, X., Foudree , A., Nambogga, M., Rodermel, S., 2007. Variegation mutants and mechanisms of chloroplast biogenesis. Plant Cell Environ. 30, 350–365.